UNIVERSITY OF CALIFORNIA

Los Angeles

Calculating Compressed Modes for Topological Crystalline Insulators

A thesis submitted in partial satisfaction

of the requirements for the degree

Master of Science in Materials Science and Engineering

by

Bradley Magnetta

2017

ABSTRACT OF THE THESIS

Calculating Compressed Modes for Topological Crystalline Insulators

by

Bradley Magnetta

Master of Science in Materials Science and Engineering

University of California, Los Angeles, 2017

Professor Vidvuds Ozoliņš, Chair

While there are many computational methods for testing the properties of topological models, most rely heavily on human intervention to produce reliable results. In theory, an approach using compressed modes would require little human intervention to calculate topological properties. We outline the computational methods needed for calculating compressed modes for a simple topological crystalline insulating model. While our methods produce accurate results we will comment on ways to further automate the standard process for calculating compressed modes by constraining topological structure.

The thesis of Bradley Magnetta is approved.

Russel Caflisch

Jaime Marian

Vidvuds Ozoliņš, Committee Chair

University of California, Los Angeles

2017

To my parents, friends, and people who have supported me.

TABLE OF CONTENTS

LIST OF FIGURES

ACKNOWLEDGMENTS

To my advisor, Professor Vidvuds Ozoliņš, thank you for your support and guidance. You have been a source of inspiration and an excellent mentor. Much thanks to all of my group members, Weston G. Nielson, Chi-Ping Liu, Jiatong Chen, Yusheng Kuo, Daniel Eth, and Junsoo Park for all your help. Finally, thank you to my additional committee members, Professor Russel Caflisch and Professor Jaime Marian.

CHAPTER 1

Introduction

1.1 Motivation

Ground breaking innovation is needed to solve imminent problems such as climate change and the physical limit to Moore's law [1]. Topological insulators are exotic materials that could contribute towards solving both of the previous mentioned crises. An experimental study has suggested that topological insulators may be feasible for use in highly efficient room-temperature devices with applications of computer memory and logic [2]. While three-dimensional (3D) topological insulators have been discovered [3] [4] further progress is needed to find practical topological insulators that are suitable for everyday use. It would be of great interest to find 3D topological insulators that are both inexpensive and effective towards alleviating world wide problems. While this search may be difficult, and beyond the construct of this thesis, refining the methods used to search for practical topological insulators is our main focus.

1.2 Topological Insulators

Duncan Haldane, winner of the 2016 Nobel prize in physics, predicted that a topological phase that mimics the quantum Hall effect (QHE) [5], can exist in a honeycomb structure where time reversal (TR) symmetry breaking effects occur [6]. This prediction was verified using a 2D HgTe quantum-well to exhibit topological properties; helical edge states [7]. TR respect-

ing topological models are the physical realization of the quantum spin Hall effect (QSHE) [8]. The Kane-Mele model [9] was the first TR respecting model to predict that a topological phase can exist in 2D honeycomb structures that include reletivistic spin effects. While the previously mentioned models are important, their 2D constraints make them impractical. Liang Fu's model for topological crystalline insulators (TCI) [10] could serve as a foundation for practical materials. In fact, TCIs have been found within the SnTe material class [4]. Not only is Fu's model 3D, but the mechanisms and interactions responsible for the topological properties are relatively simple: rotational and TR symmetry for a specific p-orbital basis.

Before we discuss methods used to study the topology of simple models it is helpful to understand the connection between a model's topology and transport. Both QHE and QSHE produce edge states with quantized ballistic transport. The nature of Quantized transport is a result of a model's invariance to a change in topology. In topological models, system properties that are invariant to changes in system energy and depend solely on the topology are called topological invariants which are constructed using wavefunctions [11]. Bernevig provides a useful derivation demonstrating the connection between QHE qunatized electron transport and a wavefunction based topological invariant in the case of Chern insulators [12].

1.3 Computational Calculations for Topological Insulators

Having identified some important scientific findings related to topological insulators it is easy to see the impact that simple tight-binding models can have on explaining experimental results. We will now discuss numerical methods used to study the topology of tight-binding models. As mentioned previously, the topological invariant is deeply connected to system wavefunctions. Thus, ideally we should be able to calculate topological properties and electron transport by calculating wavefunctions. While this seems to be a straight forward task, it has been

proven that a non-zero topological invariant is a consequence of a violation of the Stokes theorem [12]. In topological systems with non-zero quantized conductance there is no smooth gauge, choice of phase that is single valued and continuous, that can be established between system wavefunctions, making the topological invariant difficult to calculate.

The topological invariant can also be calculated using Wannier functions instead of wavefunctions. Wannier functions are obtained through a linear combination of wavefunctions using an unitary transformation which ensures that a smooth gauge is automatically established. Maximally localized Wannier functions (MLWF) [13] can be numerically calculated for a topological model, based on the groundstate wavefunction. This approach starts with pre-calculated wavefunctions and determines localized functions by minimizing the second moment [13]. However, a method based on MLWFs requires significant human intervention when selecting initial algorithm parameters and interpreting topological results due to the non-convexity of the variational problem. Another method that is based on MLWFs calculates hybrid-Wannier functions, whose charge centers can be tracked to determine topological properties [14]. While there exist many methods for obtaining the functions needed to calculate topological properties most methods rely on human intervention to get reliable results. One promising approach could involve calculating compressed modes (CM) [15]. Not only are CMs efficient to calculate but due to the convexity of their algorithm they require very little human intervention to produce reliable results. Refining our computational methods to rely less on human intervention would be helpful for studying simple tight-binding models. A more automated methodology could contribute greatly to finding practical topological insulators.

1.4 Thesis Objective and Organization

In the following chapters we will attempt to calculate the properties of a practical topological insulating model using compressed modes. While our approach produces credible results we will suggest areas where improvements can be made. This thesis will be organized in the following manner. First we will discuss the most important aspects of topological insulators and then provide details about numerically calculating CMs. We will then demonstrate how to use CMs to calculate topological properties. Next we will apply our discussion to study a simple TCI model and document calculated CMs and topological properties. Finally we will reflect on our results and conclude with some future thoughts.

References

[1] Gordon Moore. Cramming more comonents onto integrated circuits. *Electronics Magazine*, 38(8):114–117, April 1965.

[2] A. R. Mellnik, J. S. Lee, A. Richardella, J. L. Grab, P. J. Mintun, M. H. Fischer, A. Vaezi, A. Manchon, E. A. Kim, N. Samarth, and D. C. Ralph. Spin-transfer torque generated by a topological insulator. *Nature*, 511(7510):449–451, 07 2014.

[3] Haijun Zhang, Chao-Xing Liu, Xiao-Liang Qi, Xi Dai, Zhong Fang, and Shou-Cheng Zhang. Topological insulators in bi2se3, bi2te3 and sb2te3 with a single dirac cone on the surface. *Nat Phys*, 5(6):438–442, 06 2009.

[4] Timothy H. Hsieh, Hsin Lin, Junwei Liu, Wenhui Duan, Arun Bansil, and Liang Fu. Topological crystalline insulators in the snte material class. *Nature Communications*, 3:982 EP –, 07 2012.

[5] G. Dorda K. Von Klitzing and M. Pepper. New method for high-accuracy determination of the fine-structure constant based on quantized hall resistance. *Phys. Rev. Lett.*, 45(494), August 1980.

[6] F. D. M. Haldane. Model for a quantum hall effect without landau levels: Condesed-matter realization of the "parity anomaly". *Phys. Rev. Lett.*, 61(18), September 1987.

[7] B. Andrei Bernevig, Taylor L. Hughes, and Shou-Cheng Zhang. Quantum spin hall effect and topological phase transition in hgte quantum wells. *Science*, 314(5806):1757–1761, December 2006.

[8] V. I. Perel M. I. Dyakonov. Current-induced spin orientation of electrons in semiconductors. *Physics Letters A*, 35(6):459, 1971.

[9] C. L. Kane and E. J. Mele. Z2 topological order and the quantum spin hall effect. *Phys. Rev. Lett.*, 95(14):146802, September 2005.

[10] Liang Fu. Topological crystalline insulators. *Phys. Rev. Lett.*, 106(10):106802, March 2011.

[11] Taylor L. Hughes B. Andrei Bernevig. *Topological Insulators and Topological Superconductors*. Princeton University Press, 41 William Street, Princeton New Jersey 08540, 1 edition, 2013.

[12] Taylor L. Hughes B. Andrei Bernevig. *Topological Insulators and Topological Superconductors*. Number 15-32. Princeton University Press, 41 William Street, Princeton New Jersey 08540, 1 edition, 2013.

[13] Nicola Marzari and David Vanderbilt. Maximally localized generalized wannier functions for composite energy bands. *Phys. Rev. B*, 56(20):12847–12865, November 1997.

[14] Kevin F. Garrity Maryam Taherinejad and David Vanderbilt. Wannier center sheets in topological insulators. *Phys. Rev. B*, 89(115102), February 2014.

[15] Vidvuds Ozolinš, Rongjie Lai, Russel Caflisch, and Stanley Osher. Compressed modes for variational problems in mathematics and physics. *PNAS*, 110(46):18368–18373, 2013.

CHAPTER 2

Methods

2.1 Topological Analysis

2.1.1 Berry Phase

In time dependent systems, the Berry phase [1] accounts for system changes, other than the dynamical phase, that occur during quantum adiabatic transport [2]. The instantaneous eigenstates, $|n(\boldsymbol{R})\rangle$, where $\boldsymbol{R}$ is a time dependent parameter, can be used to calculate these additional changes and define the Berry phase, γ_n:

$$\gamma_n = i\int_C \langle n(\boldsymbol{R})|\nabla_{\boldsymbol{R}}|n(\boldsymbol{R})\rangle d\boldsymbol{R}. \tag{2.1}$$

The Berry phase occurs because the system is not the same at t and a later $t+dt$. More importantly, we can now define the Berry connection:

$$\boldsymbol{A}_n(\boldsymbol{R}) = i\langle n(\boldsymbol{R})|\nabla_{\boldsymbol{R}}|n(\boldsymbol{R})\rangle. \tag{2.2}$$

We refer to the Berry phase as the integral of the Berry connection along a closed curve. The Berry curvature can be written as the curl of the Berry connection, $\boldsymbol{\Omega}_n(\boldsymbol{R}) = \nabla_{\boldsymbol{R}} \times \boldsymbol{A}_n(\boldsymbol{R})$. Ref [3] demonstrates the connection between the Berry curvature and the Chern number, a topological invariant. This connection is general and demonstrates the importance of the Berry connec-

tion for analyzing the topology of a system. Topological invariants are bulk quantities that do not depend on system energies, only the system eigenfunctions [4]. This means that topological invariants are bound to the occupied band manifold, which is controlled through the opening and closing of band gaps. Furthermore, it can be shown that the Berry connection is in fact related to the Hall conductance [3] demonstrating the connection between the topological invariant and transport. Thus, systems with trivial topology will not exhibit quantized electron transport because they are in the same topological phase as the normal insulating state. Systems that break or preserve symmetries can produce non-trivial topological behavior which is characterized by quantized electron transport. Systems that rely on TR symmetry breaking to produce non-trivial behavior, such as the Chern insulator, have a topological invariant referred to as the Chern number. Other systems rely on the preservation of TR symmetry, such as the Kane-Mele model and Fu's TCI model, and are characterized by the Z_2-invariant. In fact, all TR-invariant Hamiltonians belong to the Z_2-classification. Regardless of the topological classification, all non-trivial invariants are results of a system violating the Stokes theorem through a specified portion of the first Brillouin zone (BZ). We can rewrite the Berry phase using the Stokes theorem and make a comparison to Equation 2.1. A difference occurs between these two Berry phase definitions when a topological obstruction arises as a result of the Bloch functions being non-analytic at some point in the BZ and is constrained to be an integer of 2π:

$$Z = \frac{1}{2\pi}\Big(\oint_{\partial S} \boldsymbol{A}(\boldsymbol{k})d\boldsymbol{k} - \int\int_{S} \boldsymbol{\Omega}(\boldsymbol{k})d\boldsymbol{S}\Big). \tag{2.3}$$

For non-trivial systems no global smooth gauge can be established in the BZ, for the Bloch functions, that is continuous and single valued [3]. Essentially, a non-trivial system has a set of Bloch functions with phases that are non-analytic at some point in the BZ. The symmetries that are broken or preserved in these non-trivial systems are the mechanisms which force a set of

Bloch functions to be non-analytic, and as a result violate the Stokes theorem. If the Stokes theorem is not violated, as in the trivial insulating case, then a smooth gauge can be established between the Bloch functions and no interesting electron transport will occur. This logic is easily transferable to 3D systems [5].

2.1.2 Calculating Topological Invariants

Testing the topological characteristics can be done in a few ways. We will focus on methods for calculating and testing Z_2-classification which fits with our studied model, Fu's TCI model [6]. We can apply Equation 2.2 to crystalline systems, where our eigenstates are the Bloch functions. Ref. [7] provides another equation involving the Bloch functions, called the sewing matrix,

$$B_{mn}(\boldsymbol{k}) = \langle u_m(-\boldsymbol{k}) | \, \hat{T} \, | u_n(\boldsymbol{k}) \rangle, \tag{2.4}$$

which holds all necessary topological information. Equation 2.4 considers a system where respecting only TR symmetry is necessary for non-trivial behavior. A matrix is formed by calculating $B(\boldsymbol{k})$ for each combination of the Bloch functions, u. The sewing matrix is important because it is unitary [7] and relates the Bloch functions at $\boldsymbol{k}$ and $-\boldsymbol{k}$. There exist special momenta points ($\boldsymbol{\Delta}$) in topological systems where the resulting sewing matrix value will reveal a systems topological structure. In the case of TR respecting systems these special points are TR invariant momenta (TRIM), for which $-\boldsymbol{k} = \boldsymbol{k} + \boldsymbol{G}$. At $\boldsymbol{\Delta}$-points the following relationship is true when a smooth gauge has been established throughout the BZ:

$$C(\boldsymbol{\Delta}) = \frac{\sqrt{\det B(\boldsymbol{\Delta})}}{\mathrm{Pf}[B(\boldsymbol{\Delta})]} = \pm 1. \tag{2.5}$$

For a (2×2) sewing matrix, the Pfaffian reduces to $\mathrm{Pf}[B(\boldsymbol{k})] = B_{12}(\boldsymbol{k})$. The topological character, or in this case the Z_2-index can be calculated for a system by taking the product of C at all $\boldsymbol{\Delta}$-points. If the resulting product is -1 then our system has non-trivial topological behavior because this represents a winding in phase due to a violation of the Stokes theorem. Some Z_2 topological models require additional symmetry to produce non-trivial behavior. In the case of Fu's TCI model, both C_4 and TR symmetry must be preserved and a corresponding sewing matrix would include both symmetries in its formulation.

Topological analysis can also be done using Wannier functions. The Bloch functions and Wannier functions, W, are related through a Fourier transform,

$$u_n(\boldsymbol{k}) = \sum_{\boldsymbol{R}} e^{i\boldsymbol{k}\boldsymbol{R}} W_n(\boldsymbol{r} - \boldsymbol{R}). \tag{2.6}$$

We can construct a real space matrix similar to Equation 2.4 by imposing symmetry relations between Wannier functions. Here we consider a model that respects only TR symmetry:

$$U_{mn}(\boldsymbol{r}) = \langle W_m(\boldsymbol{r} - \boldsymbol{R}) | \hat{T} | W_n(0) \rangle. \tag{2.7}$$

In order to calculate topological properties, we must Fourier transform $U(\boldsymbol{r})$, obtaining a sewing-like matrix $U(\boldsymbol{k})$. We can use $U(\boldsymbol{k})$ to determine topological structure by taking the following contour integral about half the BZ, in the case of Z_2 classification:

$$I = \frac{1}{2\pi i} \oint_C \nabla_{\boldsymbol{k}} \log[U_{21}(\boldsymbol{k}) + i\delta_{\boldsymbol{k}}] d\boldsymbol{k}. \tag{2.8}$$

Here, we sum up all imaginary portions of $U(\boldsymbol{k})$ phase which is analogous to the Berry phase. This procedure results in a value I which we call our Z_2-invariant. The path chosen will incorpo-

rate a system's $\boldsymbol{\Delta}$-points but must be a continuous loop. As we move along our path it is possible that $U(\boldsymbol{k}) = 0$. Thus, we have incorporated $i\delta_{\boldsymbol{k}}$ into our integrand to avoid such undefined terms.

2.2 Topological Crystalline Insulators

Studying practical topological models could be the key to finding real topological materials for everyday use. Liang Fu first suggested the topological crystalline insulator (TCI) [6] which demonstrates how non-trivial topological behavior can arise in crystalline systems without relativistic spin-orbit effects. We will now discuss Fu's TCI model in detail.

2.2.1 Fu's TCI Model

Fu's TCI model respects both crystal point group symmetries and TR symmetry. In this case TR symmetry operator is represented by complex conjugation. One advantage of the TCI model is that it is a spin-less system, which does not rely on spin-orbital coupling to produce non-trivial behavior. Instead, the TCI model relies on p-orbitals which act like pseudo-spins to produce an effect similar to QSHE. The TCI model is based on a tetragonal crystal with C_4 symmetry, including a unit cell of two inequivalent atoms A and B along a c-axis as shown in Figure 2.1.A. Only the p_x and p_y orbitals are necessary to study the topological behavior [6] making our primitive cell fairly simple. We can Fourier transform Fu's tight-binding model to obtain the $\boldsymbol{k}$-space Hamiltonian; a required input for calculating CMs as shown in Figure 2.3:

$$H(\boldsymbol{k}) = \begin{pmatrix} \mathrm{H}^{A}(\boldsymbol{k}) & \mathrm{H}^{AB}(\boldsymbol{k}) \\ \mathrm{H}^{AB\dagger}(\boldsymbol{k}) & \mathrm{H}^{B}(\boldsymbol{k}) \end{pmatrix}, \tag{2.9}$$

$$H^a(\boldsymbol{k}) = 2t_1^a I + 2t_2^a \begin{pmatrix} \cos(k_x)\cos(k_y) & \sin(k_x)\sin(k_y) \\ \sin(k_x)\sin(k_y) & \cos(k_x)\cos(k_y) \end{pmatrix}, \tag{2.10}$$

$$H^{AB}(\boldsymbol{k}) = [t_1' + 2t_2'(\cos(k_x) + \cos(k_y)) + t_z' e^{ik_z}]I. \tag{2.11}$$

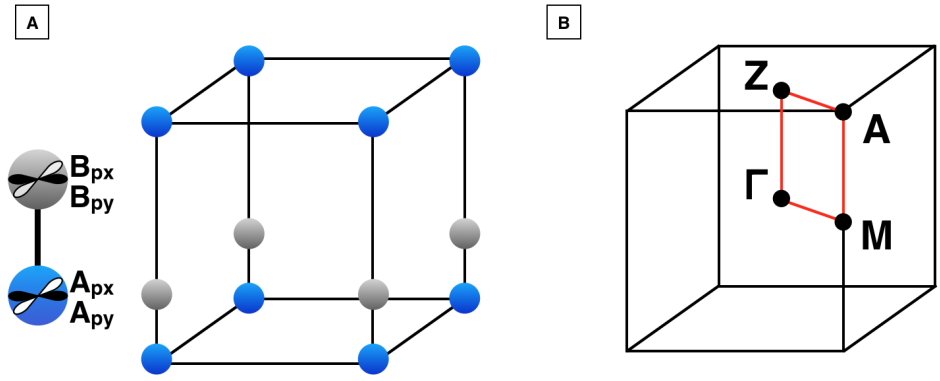

Figure 2.1: A) Tetragonal crystal structure with a basis consisting of two inequivalent atoms and p-orbtials. B) High symmetry path within the first Brillouin zone.

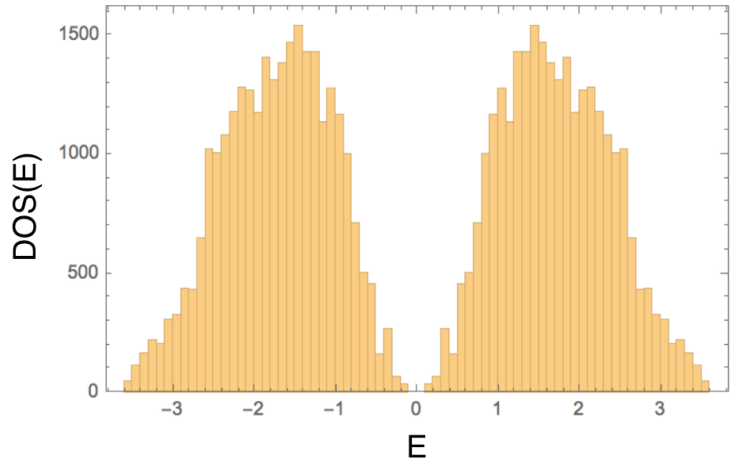

Figure 2.2: Density of states for Fu's TCI model [6]; $N = 24$, $E_T = 3.4482$, $E_{gap} = 0.353773$

Where the parameter a refers to either atom choice, A or B. Equation 2.9 includes nearest and next-nearest neighbor intralayer hoppings in H^a and interlayer hoppings in H^{AB}. Fu suggests using the following system parameter values to study the non-trivial phase: $t_1^A = -t_1^B = 1$,

$t_2^A = -t_2^B = 0.5$, $t_1^{'} = 2.5$, $t_2^{'} = 0.5$, $t_z^{'} = 2$. We can study the density of states from our Bloch Hamiltonian by creating an $(N \times N \times N)$ super-lattice, as represented by Figure 2.2. The density of states reveals both the total energy and band gap of the corresponding super-lattice. Fu identifies four special momenta points $\boldsymbol{\Gamma} = (0,0,0)$, $\boldsymbol{M} = (\pi,\pi,0)$, $\boldsymbol{A} = (\pi,\pi,\pi)$, and $\boldsymbol{Z} = (0,0,\pi)$. The path $(\boldsymbol{\Gamma} - \boldsymbol{M} - \boldsymbol{A} - \boldsymbol{Z} - \boldsymbol{\Gamma})$ can be used to define the contour integral in Equation 2.8 to determine the topological nature of the studied TCI system. If trivial topology is present the contour integral will result in an even integer of 2π. If non-trivial topology is present the contour integral will result in an odd integer of 2π. We will use our algorithm to obtain CMs that describe the valance bands of the TCI model. These CMs will have the following basis for each super-cell lattice site, $\left\{A_{p_x}, A_{p_y}, B_{p_x}, B_{p_y}\right\}$.

2.3 Compressed Modes

In order to calculate the properties of a topological model in an automated manner it is not enough to calculate a system's Bloch functions. Any methods involving the Bloch functions will require a smooth gauge throughout the BZ. However, as we have mentioned non-trivial behavior results in the inability to establish a smooth gauge that satisfies all Bloch functions simultaneously while preserving symmetry. This makes calculating non-trivial properties from the Bloch functions a difficult problem. One method to remove the burden of having to establish a smooth gauge is to use Wannier functions as the root of our topological analysis. We will discuss a set of functions that not only remove the burden of establishing a smooth gauge but are better suited for an automated process; compressed modes (CM) [8].

2.3.1 Mathematical Description

The independent-particle Shrödinger equation, without spin effects, can be expressed using the following variational problem [8],

$$E_0 = \min_{\Phi} \sum_{j=1}^{N} \langle \phi_j | \hat{H} | \phi_j \rangle \quad \text{s.t.} \quad \langle \phi_j | \phi_k \rangle = \delta_{jk}, \tag{2.12}$$

Where $\hat{H}$ is the Hamiltonian, E_0 is the groundstate energy, and $\Phi = \{\phi_i\}_{i=1}^{N}$ is a collection of orthonormal functions that span the N-eigenspace of $\hat{H}$. Through diagonalization of $\langle \phi_j | \hat{H} | \phi_j \rangle$ we can obtain eigenfunctions $\Psi = \{\psi_i\}_{i=1}^{N}$, which are usually used to produce a set of spatially localized functions that span the occupied eigenspace of $\hat{H}$ [8]:

$$W_i(\boldsymbol{r}) = \sum_j U_{ij} \psi_j(\boldsymbol{r}). \tag{2.13}$$

U must be unitary and is responsible for a subspace rotation of the system eigenfunctions. These functions are often referred to as Wannier functions [9], but there are many choices of U that can produce sparse solutions that still span the occupied eigenspace of $\hat{H}$. Here we use the term sparse to refer to localized solutions with compact support. While there exist many methods for determining W_j [10], calculating CMs have advantages conducive towards automation. The CM method introduces L_1-regularization into the above variational problem (Eqn. 2.12) to approximate the total energy while simultaneously producing sparse solutions without the need to calculate the eigenfunctions [8]:

$$E = \min_{\Phi} \sum_{j=1}^{N} \left(\frac{1}{\mu} |\phi_j|_1 + \langle \phi_j | \hat{H} | \phi_j \rangle \right) \quad \text{s.t.} \quad \langle \phi_j | \phi_k \rangle = \delta_{jk}. \tag{2.14}$$

Essentially, CMs rely on the L_1-penalty term to choose a value for U that produces sparse solu-

tions. The parameter μ controls a trade off between localization and energy. Choosing a large value for μ will effectively reduce Equation 2.14 to Equation 2.12. As a result, we will obtain delocalized solutions that have good total energy approximation. Choosing a small value for μ will introduce a large L_1-norm presence and result in very localized solutions with bad total energy approximation. A discretized version of Equation 2.14 can be solved numerically by splitting the orthogonality constraint (SOC) as discussed in Ref. [11].

2.3.2 Computational Algorithm

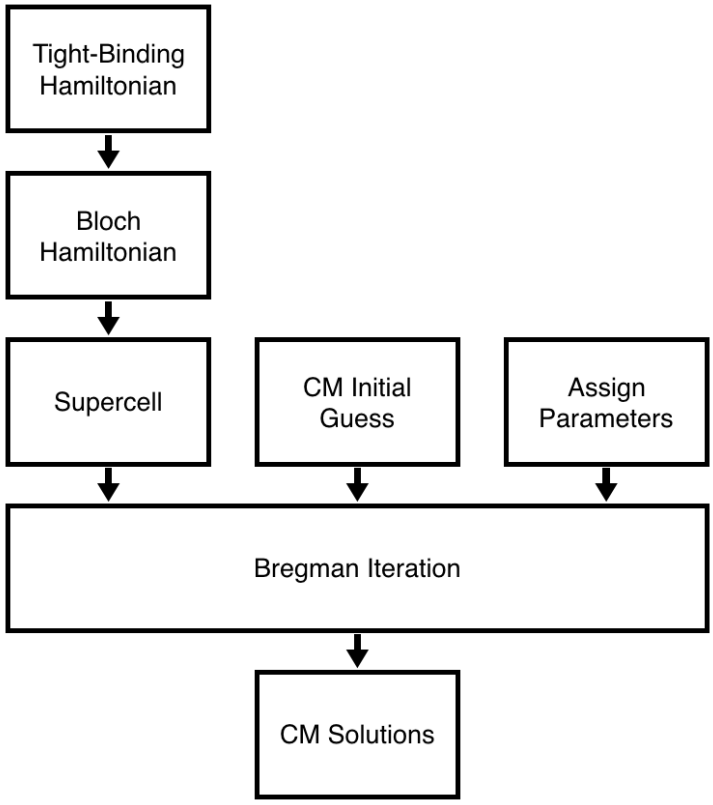

Figure 2.3: Computational flow used to calculate CMs for a tight-binding model.

Figure 2.3 describes the computational flow we use in our algorithm to solve Equation 2.14 [11]. From a tight-binding Hamiltonian we can apply a Fourier transform to produce a Bloch Hamiltonian; this process is commonly done analytically. We can construct a $\boldsymbol{k}$-space

Hamiltonian, $\hat{H}_k$, that is representative of a square ($N \times N \times N$) sized super-cell. Our algorithm must be initialized with the following: $\hat{H}_k$, an initial guess for our CMs, and Bregman iteration parameters [11]. In our calculations we fix the following Bregman parameters: $\lambda = \gamma = 10$. We've set the number of iterations per algorithm instance to $I = 40$ which should be enough to arrive at approximate minimum solutions. μ is the parameter that controls the trade off between band structure accuracy and localization, and was varied between $\mu_R = [25 : 500]$ to produce CMs with non-trivial topological structure. We choose a $N = 24$ super-cell size to ensure our CMs are contained within the super-cell lattice.

2.3.3 CM Initial Guess

As mentioned previously, in order to execute our algorithm we need to define an initial guess for our CMs. Incorporating an L_1-penalty term into the variational problem, Equation 2.14, introduces convexity [8]. This makes our initial guess for the CMs less important because regardless of how we initialize the problem our algorithm is less likely to get trapped by local minimum solutions. While our work does not define a procedure to guarantee accurate solutions for all tight-binding Hamiltonians, the following methods helped us produce reliable CMs for the Fu TCI model. Wannier fuctions are exponentially localized in 2D and 3D, except for Chern insulators [12]. Thus, a simple approach to choosing a CM initial guess is to use a random exponentially decaying function positioned at the center of our super-cell,

$$\psi^0_{\text{in}}(\boldsymbol{r}) = (1+i)Re^{-|\boldsymbol{r}-\boldsymbol{r}_c|}. \tag{2.15}$$

Equation 2.15, demonstrates our random initialization where $\boldsymbol{r}$ is the lattice position, $\boldsymbol{r}_c$ is the central lattice position, and R is a random number chosen between $[-1 : 1]$. Our initial guess should have the same topological structure as our desired result. If it does not, we will not arrive

at CMs that accurately represent the studied model. While an initial guess structure can be determined analytically for a model, random initialization along with a trial and error approach is sufficient for numerical topological analysis.

2.3.4 Wannier Interpolation

Having discussed methods for calculating CMs for a given tight-binding model, it is important to verify the accuracy of these CM solutions. Accurate CMs not only approximate total energy but can also be used to recreate the band structure. Comparing the total energy and band structure of the tight-binding model against the total energy and band structure produced by CMs will help determine CM accuracy. We can obtain the band structure from our CMs through a Wannier interpolation. We start by Fourier transforming our CMs into momentum-space, resulting in the Bloch functions described by equation 2.6. We form a matrix of inner products using our Bloch functions and our Bloch Hamiltonian:

$$M_{ij}(\boldsymbol{k}) = \langle u_i | H(\boldsymbol{k}) | u_j \rangle. \tag{2.16}$$

For the case of Fu's TCI model, $H(\boldsymbol{k})$ is defined by Equation 2.9. It is more beneficial to convert $M_{ij}(\boldsymbol{k})$ into real-space and is done so through a Fourier Transform, $M_{ij}(\boldsymbol{r}) = \sum_{\boldsymbol{k}} M_{ij}(\boldsymbol{k}) e^{-i2\pi \boldsymbol{k}\boldsymbol{r}}$. Through a final Fourier Transform of $M(\boldsymbol{r})$ we can obtain $M(\boldsymbol{k})$ at any point in momentum-space. We can diagonalize $M(\boldsymbol{k})$ using an invertible unitary matrix X to obtain a diagonal matrix D,

$$X^{\dagger} M(\boldsymbol{k}) X = D. \tag{2.17}$$

Eigenvalues are obtained from the diagonal elements of D, $\lambda = \{D_{ii}\}_{i=1}^{N_D}$; where D is a square

matrix of order N_D . We can now build an interpolated band structure using λ along a specified momentum path. In the case of Fu's TCI model the momentum path of interest is ($\boldsymbol{\Gamma} - \boldsymbol{M} - \boldsymbol{A} - \boldsymbol{Z} - \boldsymbol{\Gamma}$), as depicted in Figure 2.1.B.

2.3.5 μ-dependence

Another way to test the accuracy of our CM solutions is by checking the convergence of the total energy and the L_1-norm with respect to a change in the parameter μ. Non-trivial CMs with Z_2-classification will have an L_1-norm that varies as μ^{-2} and a total energy that varies linearly [8] (Figure 2.4). Figure 2.5 demonstrate the computational flow that is used to test a solution's μ-dependence.

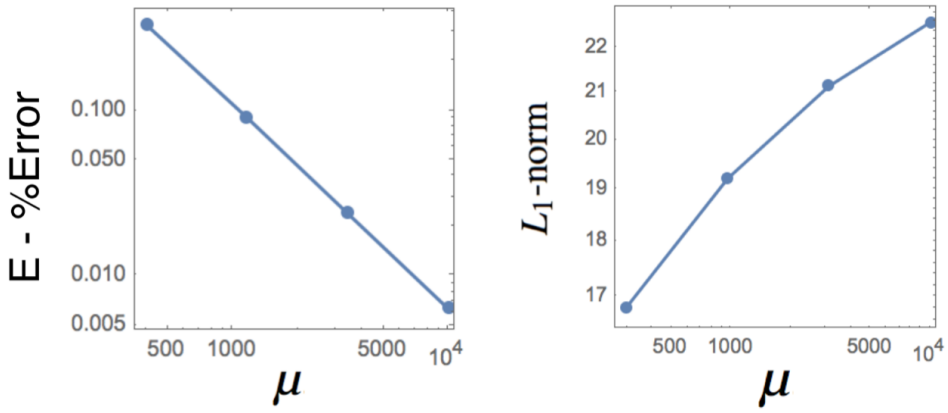

Figure 2.4: An example μ-dependence for CMs with non-trivial topology. A) the desired total energy, E, variation to increasing μ, B) the desired L_1-norm variation to an increasing μ.

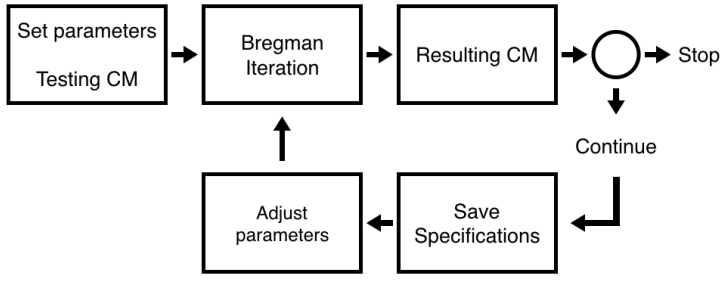

Figure 2.5: Computational flow for determining CM μ-dependence.

References

[1] M. V. Berry. Quantal phase factors accompanying adiabatic changes. *Proc. R. Soc. Lond.*, 392:45, 1984.

[2] Taylor L. Hughes B. Andrei Bernevig. *Topological Insulators and Topological Superconductors*. Number 6-8. Princeton University Press, 41 William Street, Princeton New Jersey 08540, 1 edition, 2013.

[3] Taylor L. Hughes B. Andrei Bernevig. *Topological Insulators and Topological Superconductors*. Number 15-32. Princeton University Press, 41 William Street, Princeton New Jersey 08540, 1 edition, 2013.

[4] Taylor L. Hughes B. Andrei Bernevig. *Topological Insulators and Topological Superconductors*. Princeton University Press, 41 William Street, Princeton New Jersey 08540, 1 edition, 2013.

[5] Taylor L. Hughes B. Andrei Bernevig. *Topological Insulators and Topological Superconductors*. Number 144. Princeton University Press, 41 William Street, Princeton New Jersey 08540, 1 edition, 2013.

[6] Liang Fu. Topological crystalline insulators. *Phys. Rev. Lett.*, 106(10):106802, March 2011.

[7] Taylor L. Hughes B. Andrei Bernevig. *Topological Insulators and Topological Superconductors*. Number 143. Princeton University Press, 41 William Street, Princeton New Jersey 08540, 1 edition, 2013.

[8] Vidvuds Ozolinš, Rongjie Lai, Russel Caflisch, and Stanley Osher. Compressed modes for variational problems in mathematics and physics. *PNAS*, 110(46):18368–18373, 2013.

[9] G. H. Wannier. The structure of electronic excitation levels in insulating crystals. *Phys Rev*, 3(52):191–197, 1937.

[10] Nicola Marzari and David Vanderbilt. Maximally localized generalized wannier functions for composite energy bands. *Phys. Rev. B*, 56(20):12847–12865, November 1997.

[11] Stanley Osher Rongjie Lai. A splitting method for orthogonality constrained problems. *J Sci Comput*, 58:431–449, May 2013.

[12] Matteo Calandra Christophe Mourougane Nicola Marzari Christian Brouder, Gianluca Panati. Exponential localization of wannier functions in insulators. *Phys. Rev. Lett.*, 98(4):046402, January 2007.

CHAPTER 3

Compressed Modes for Topological Crystalline Insulators

All results discussed in this section use the methods and parameter settings described in chapter 2 to calculate and analyze CMs from a TCI super-cell Bloch Hamiltonian. We will produce CMs that accurately represent total energy, desired sparsity, and non-trivial topology.

3.1 Trivial Compressed Modes

We demonstrate CM results obtained from initializing our algorithm using Equation 2.15 and executing our algorithm [1] a single instance setting $\mu = 100$. The resulting CMs, W_{even}, produce an inaccurate interpolated band structure (Fig.3.1). The plot in Figure 3.2 was created by building a unitary matrix from W_{even}, (Eqn. 2.7), and calculating the topological invariant using Equation 2.8; carrying out the contour integral along the path ($\boldsymbol{\Gamma} - \boldsymbol{M} - \boldsymbol{A} - \boldsymbol{Z} - \boldsymbol{\Gamma}$) [2]. We see that the contour integral is approximately zero, an even integer of 2π, proving W_{even} exhibits trivial topological behavior.

3.2 Non-trivial Compressed Modes

We demonstrate CM results obtained from initializing our algorithm using Equation 2.15 and executing our algorithm [1] a single instance setting $\mu = 400$. The resulting CMs, W_{odd}, produce an accurate interpolated band structure (Fig.3.3).

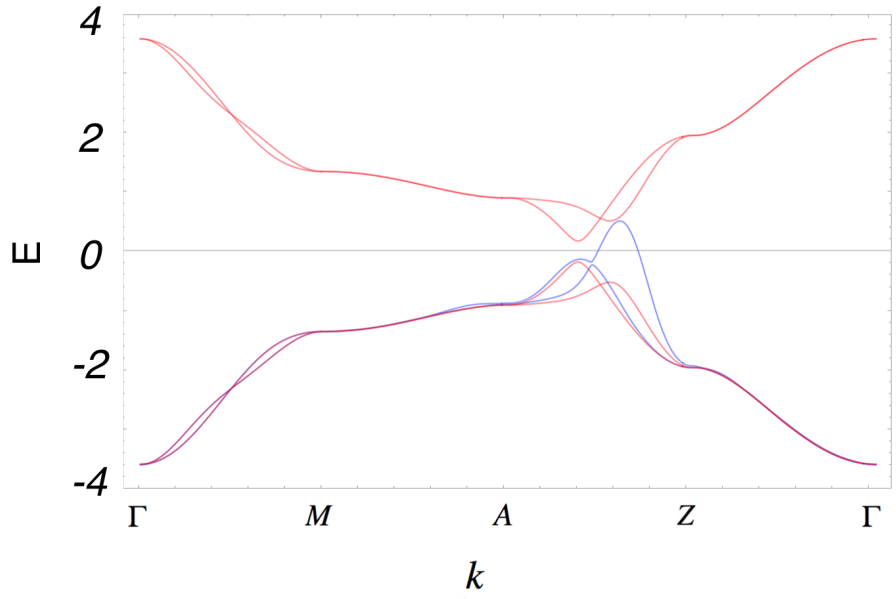

Figure 3.1: The red plot represents the band structure obtained from the Bloch Hamiltonian of the Fu TCI model, while the blue plot represents a Wannier interpolated band structure of W_{even}; $\mu = 100$.

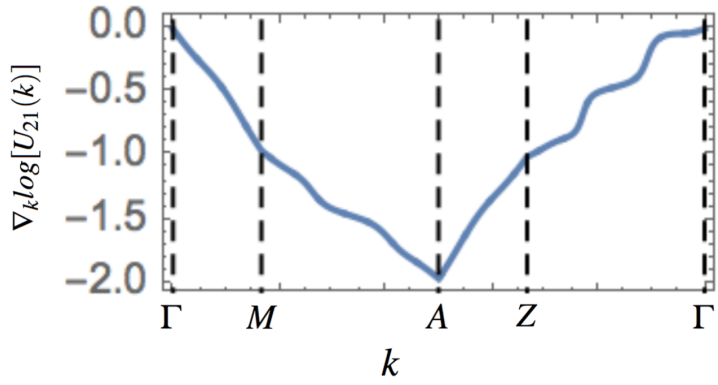

Figure 3.2: Tracking the contour integral as described by Equation 2.8 for W_{even}. The sum of the blue plot reveals a trivial topological invariant of $I = 0.000154892$

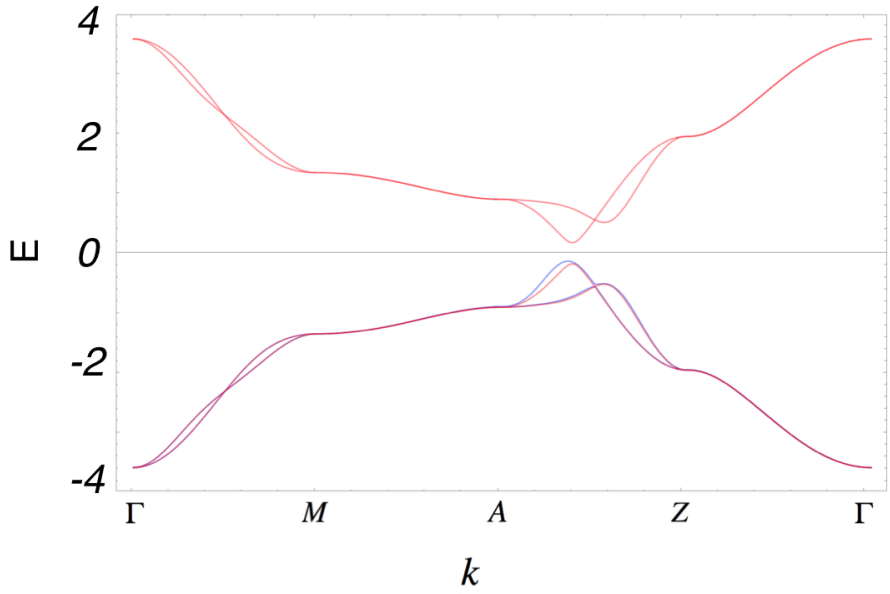

Figure 3.3: The red plot represents the band structure obtained from the Bloch Hamiltonian of the Fu TCI model, while the blue plot represents a Wannier interpolated band structure of W_{odd}; $\mu = 400$.

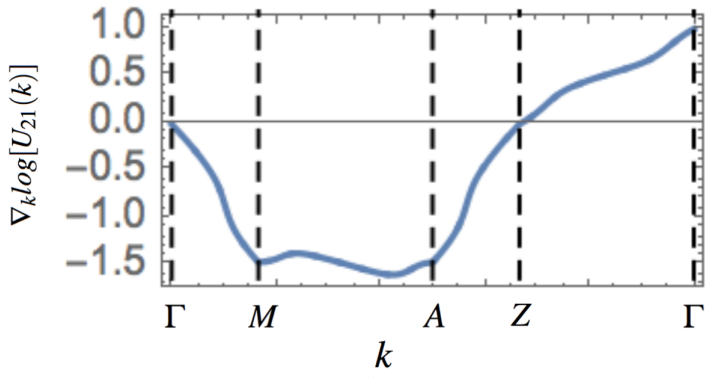

Figure 3.4: Tracking the contour integral as described by Equation 2.8 for W_{odd}. The sum of the blue plot reveals an odd topological invariant of $I = 1$

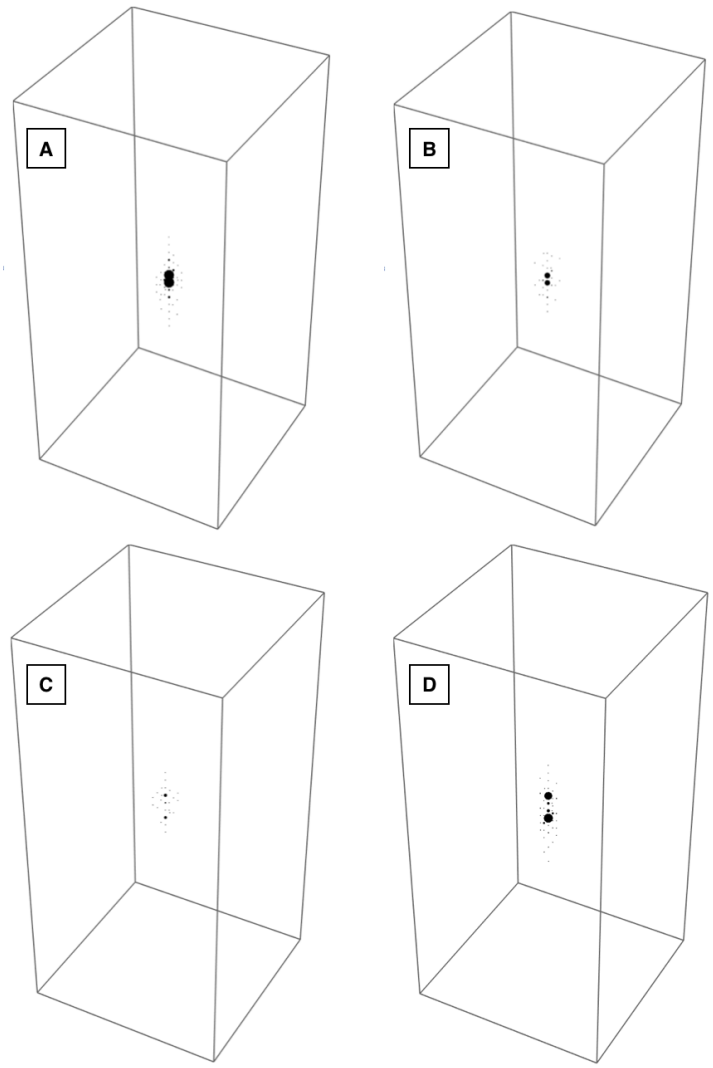

Figure 3.5: Compressed mode 3D plot. A) Re$[\Psi_{1p_x}]$. B) Im$[\Psi_{1p_x}]$. C) Re$[\Psi_{1p_y}]$. D) Im$[\Psi_{1p_y}]$

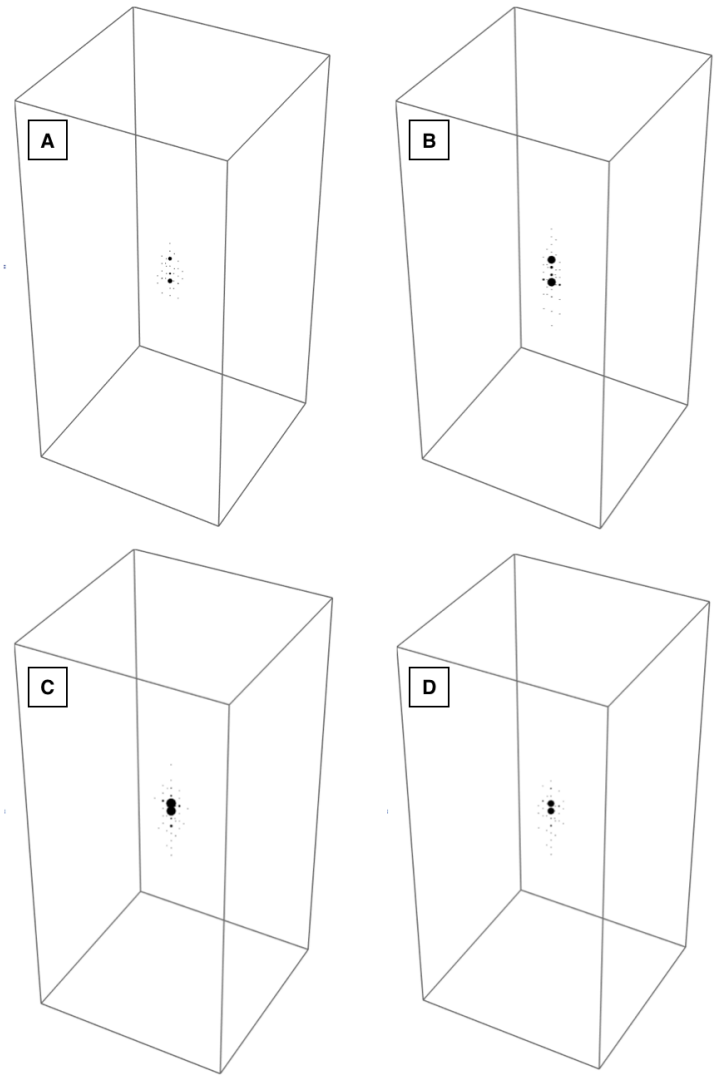

Figure 3.6: Compressed mode 3D plot. A) Re$[\Psi_{2p_x}]$. B) Im$[\Psi_{2p_x}]$. C) Re$[\Psi_{2p_y}]$. D) Im$[\Psi_{2p_y}]$

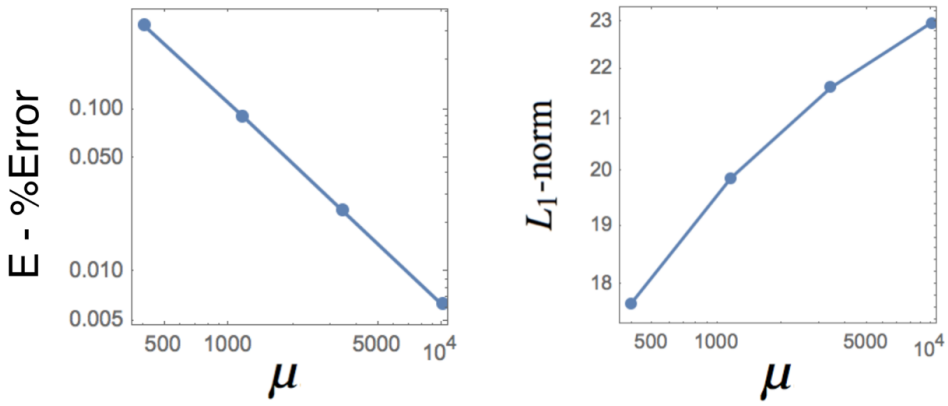

Figure 3.7: W_{odd} μ-dependence. Using Figure 2.4 as a reference we can classify W_{odd} as having non-trivial μ-dependence A) a negative linear slope with increase μ. B) a slope following μ^{-2} with increasing μ.

The plot in Figure 3.4 was created by building a unitary matrix from W_{odd}, (Eqn. 2.7), and calculating the topological invariant using Equation 2.8; carrying out the contour integral along the path ($\boldsymbol{\Gamma} - \boldsymbol{M} - \boldsymbol{A} - \boldsymbol{Z} - \boldsymbol{\Gamma}$) [2]. We see that the contour integral results in unity, an odd integer of 2π, proving W_{odd} exhibits non-trivial topological behavior. We can visualize W_{odd} by plotting amplitude over the whole super-cell for each basis component as shown by Figures 3.5 and 3.6. Our 3D plots represent the absolute value of the amplitude at a lattice point by the size of the sphere. Only absolute value amplitudes that are greater than a threshold value of 0.01 are shown. The 3D plots cover all lattice sites including both A and B atoms, but we will have to break each CM into four subplots to fully visualize the real, imaginary, p_x-orbital, and p_y-orbital components. The amplitude in Figures 3.5 and 3.6 is contained within our super-cell and localized at the central lattice position. Besides quantifying accuracy using the total energy, topology, and sparsity of W_{odd}, we can also check how W_{odd} varies to changing μ to test the accuracy of CMs. More specifically, the μ-dependence of W_{odd} will verify that we have retrieved CMs with non-trivial topology. We make this claim by comparing Figures 2.4 and 3.7.

3.3 Discussion

We have discussed a variety of numerical methods that can be used to produce CMs for Fu's TCI model that accurately represent the Bloch Hamiltonian band structure and produce the correct topological character. However, our computational process required human intervention and chance for proper initialization of our algorithm. It would be very useful to append the common method for calculating CMs [3] to ensure the correct topological structure is retrieved while simultaneously minimizing the total energy and producing sparse solutions. If this were possible through an additional penalty term, as was done with the L_1-norm to ensure sparsity, the procedure for obtaining accurate CMs with the correct topology would become very automated.

References

[1] Stanley Osher Rongjie Lai. A splitting method for orthogonality constrained problems. *J Sci Comput*, 58:431–449, May 2013.

[2] Liang Fu. Topological crystalline insulators. *Phys. Rev. Lett.*, 106(10):106802, March 2011.

[3] Vidvuds Ozolinš, Rongjie Lai, Russel Caflisch, and Stanley Osher. Compressed modes for variational problems in mathematics and physics. *PNAS*, 110(46):18368–18373, 2013.